

Spin freezing in the van der Waals material $Mn_2Ga_2S_5$

Jie Shen(沈洁), Xitong Xu(许锡童), Miao He(何苗), Yonglai Liu(刘永来), Yuyan Han(韩玉岩), and Zhe Qu(屈哲)
Citation: Chin. Phys. B, 2022, 31 (**6**): 067105. DOI: 10.1088/1674-1056/ac657c
Journal homepage: http://cpb.iphy.ac.cn; http://iopscience.iop.org/cpb

What follows is a list of articles you may be interested in

Doublet luminescence due to coexistence of excitons and electron-hole plasmas in optically excited $CH_3NH_3PbBr_3$ single crystal

Jie Wang(王杰), Guang-Zhe Ma(马广哲), Lu Cao(曹露), Min Gao(高敏), and Dong Shi(石东)
Chin. Phys. B, 2022, 31 (**4**): 047104. DOI: 10.1088/1674-1056/ac29b5

Review of Raman spectroscopy of two-dimensional magnetic van der Waals materials

Yu-Jia Sun(孙宇伽), Si-Min Pang(庞思敏), and Jun Zhang(张俊)
Chin. Phys. B, 2021, 30 (**11**): 117104. DOI: 10.1088/1674-1056/ac1e0f

Interfacial properties of g-C_3N_4/TiO_2 heterostructures studied by DFT calculations

Chen-Shan Peng(彭春山), Yong-Dong Zhou(周永东), Sui-Shuan Zhang(张虽栓), and Zong-Yan Zhao(赵宗彦)
Chin. Phys. B, 2021, 30 (**1**): 017101. DOI: 10.1088/1674-1056/abb30b

Intercalation of van der Waals layered materials: A route towards engineering of electron correlation

Jingjing Niu(牛晶晶), Wenjie Zhang(章文杰), Zhilin Li(李治林), Sixian Yang(杨嗣贤), Dayu Yan(闫大禹), Shulin Chen(陈树林), Zhepeng Zhang(张哲朋), Yanfeng Zhang(张艳锋), Xinguo Ren(任新国), Peng Gao(高鹏), Youguo Shi(石友国), Dapeng Yu(俞大鹏), Xiaosong Wu(吴孝松)
Chin. Phys. B, 2020, 29 (**9**): 097104. DOI: 10.1088/1674-1056/abab85

Hubbard model on an anisotropic checkerboard lattice at finite temperatures: Magnetic and metal-insulator transitions

Hai-Di Liu(刘海迪)
Chin. Phys. B, 2019, 28 (**10**): 107102. DOI: 10.1088/1674-1056/ab4279

RAPID COMMUNICATION

Spin freezing in the van der Waals material $Mn_2Ga_2S_5$

Jie Shen(沈洁)[1,2], Xitong Xu(许锡童)[1], Miao He(何苗)[1,2], Yonglai Liu(刘永来)[1,2], Yuyan Han(韩玉岩)[1,2], and Zhe Qu(屈哲)[1,2,†]

[1] *Anhui Province Key Laboratory of Condensed Matter Physics at Extreme Conditions, CAS Key Laboratory of Photovoltaic and Energy Conservation Materials, High Magnetic Field Laboratory, Hefei Institutes of Physical Science, Chinese Academy of Sciences, Hefei* 230031, *China*

[2] *Science Island Branch of Graduate School, University of Science and Technology of China, Hefei* 230026, *China*

(Received 16 March 2022; revised manuscript received 23 March 2022; accepted manuscript online 8 April 2022)

Geometrical frustration in low-dimensional magnetic systems has been an intriguing research aspect, where the suppression of conventional magnetic order may lead to exotic ground states such as spin glass or spin liquid. In this work we report the synthesis and magnetism study of the monocrystalline $Mn_2Ga_2S_5$, featuring both the van der Waals structure and a bilayered triangular Mn lattice. Magnetic susceptibility reveals a significant antiferromagnetic interaction with a Curie–Weiss temperature $\theta_w \sim -260$ K and a high spin $S = 5/2$ Mn^{2+} state. However, no long range magnetic order has been found down to 2 K, and a spin freezing transition is found to occur at around 12 K well below its θ_w. This yields a frustration index of $f = -\theta_w/T_f \approx 22$, an indication that the system is highly frustrated. The absence of a double-peak structure in magnetic specific heat compared with the TM_2S_4 compounds implies that the spin freezing behavior in $Mn_2Ga_2S_5$ is a result of the competition between exchange interactions and the 2D crystalline structure. Our results suggest that the layered $Mn_2Ga_2S_5$ would be an excellent candidate for investigating the physics of 2D magnetism and spin disordered state.

Keywords: geometrical frustration, van der Waals material, spin freezing

PACS: 71.20.Nr, 75.50.−y, 75.50.Lk **DOI:** 10.1088/1674-1056/ac657c

1. Introduction

Geometrical frustration, defined as situations where interactions between neighboring spins cannot be energy-minimized simultaneously,[1] often appears in triangular, face-centered cubic, hexagonal close-packed and kagome lattices.[2–6] Such geometrical frustration can lead to many novel phenomena by suppressing conventional magnetic orders,[7–10] including highly degenerate ground states, strong fluctuations, cooperative paramagnetism, spin disordered state at low temperature, etc.[11–16] In particular, the triangular lattice in two dimensions (2D) is the simplest and the first proposed structure of geometrical frustrated systems due to a single magnetic ion per unit cell.[17] A lot of three-dimensional materials with triangular magnetic lattice have been investigated, such as Gd_2PdSi_3,[18] $CuFeO_2$,[19] $LuCoGaO_4$,[20] and $Ca_3CoNb_2O_9$,[21] but only a few van der Waals (vdWs) triangular magnets have been investigated, where the interplay of low dimensionality and spin frustration may lead to the emergence of exotic physical properties.

The TM_2X_4 (T = Ni/Fe; M = Ga/Al; X = S/Se) is one of the few systems that possess the vdWs 2D triangular geometry with the magnetic transition metal sublattice. Among them, $NiGa_2S_4$ is a typical bulk-insulating antiferromagnet with an exact triangular lattice. Combined magnetic susceptibility, specific heat and neutron-diffraction experiments have shown no long-range order; instead nanoscale quasi-static correlation is found, indicating that geometrical frustration can stabilize a low temperature spin disordered state with coherence beyond the two-spin correlation length.[2,22,23] The magnetic specific heat at low temperatures shows T^2 power law, indicating a 2D gapless linearly dispersive mode.[24] The isostructural $FeGa_2S_4$ and $FeAl_2Se_4$, where the transition Fe^{2+} ion has a spin $S = 2$ that is twice larger than $S = 1$ for Ni^{2+}, exhibit a similar spin disordered state at low temperatures.[25–28] It is further suggested that the integer spin size is crucial for the existence of such spin wave excitations, since Zn^{2+} ($S = 0$) and Fe^{2+} ($S = 2$) substitutions in $NiGa_2S_4$ retain the same feature while Co^{2+} or Mn^{2+} substitution does not.[29]

Instead of substituting the basal transition metal, an alternative way is to explore the quantum physics of the bilayer system in the related compounds.[24,30–32] $Fe_2Ga_2S_5$ is the homologous compound of TM_2X_4. The bilayer Fe atoms form a kind of distorted honeycomb lattice with strong super-exchange interaction mediated by sulfur, leading to a long-range antiferromagnetic order at $T_N = 113$ K.[24,33] Based on the difference between the 124 and 225 compounds, it was suggested that geometrical frustration in quasi-2D triangular systems is crucial for the spin disordered state.[24] However, whether bilayer $T_2M_2X_5$ systems or half-odd integer spins exclude these spin-disordered states remains an open question.

†Corresponding author. E-mail: zhequ@hmfl.ac.cn

© 2022 Chinese Physical Society and IOP Publishing Ltd

In order to investigate bilayering effect and half-odd integer spin in stabilizing the spin disordered state, we searched and have succeeded in synthesizing single crystals of the homologous $Mn_2Ga_2S_5$. Using combined magnetism and heat capacity measurements, we find that $Mn_2Ga_2S_5$ exhibits a spin freezing transition at 12 K, well below its $\theta_w \sim -260$ K. This spin freezing behavior is a result of the competition between exchange interactions and the bilayered 2D crystalline structure. Our results suggest that the layered $Mn_2Ga_2S_5$ would be a good candidate for investigating the physics of 2D magnetism and spin disordered state.

2. Experimental method

Single crystals of $Mn_2Ga_2S_5$ are synthesized by the chemical vapor transport (CVT) method. High-purity elements Mn, Ga and S with stoichiometric molar ratio of 2 : 2 : 5 are mixed and put into the quartz ampoule. Iodine (3 mg/cm^3) is used as the transport agent. The ampoule is vacuum sealed and placed in a two-temperature-zone tube furnace with a temperature gradient of 1050–950 °C for 7 days, then cooled down to room temperature naturally. As shown in the inset of Fig. 1(c), large amounts of dark brown single crystals which are soft and easily exfoliated can be obtained for each trial. Direct reaction of the stoichiometric elements at 1050 °C also leads to the formation of well faceted crystals, yet they always encapsule large amounts of unreacted sulfur.

Crystals grown by CVT are grounded into powder for the x-ray diffraction (XRD) characterization. XRD patterns are collected at room temperature on a Rigaku MiniFlex powder diffractometer using filtered Cu-K_α radiation. The chemical composition of Mn:Ga:S is also measured by energy dispersive x-ray (EDX) spectrum. The dc and ac magnetic susceptibilities are measured from room temperature down to 2 K with a superconductive quantum interference device (SQUID). Specific heat of $Mn_2Ga_2S_5$ single crystals is mainly characterized in a Quantum Design physical property measurement system (PPMS-14T).

3. Results and discussion

$Mn_2Ga_2S_5$ belongs to the space group $P\bar{3}m1$. As shown in Fig. 1, it possesses a layered triangular structure that can be described as slabs of two GaS layers and one central Mn_2S_3 layer. The Mn^{2+} ion, forming two sets of triangle sublattice, adopts an electronic configuration $t_{2g}^3 e_g^2$ that gives rise to a high spin state with $S = 5/2$ local moment. The top and bottom sheets of GaS_4 tetrahedra are connected by the central Mn_2S_3 layer of edge-sharing MnS_6 octahedra. Along the crystallographic c direction, the tri-layered unit is separated by typical vdWs gaps. Figure 1(c) shows EDX results of our single crystals. The element molar ratio of Mn : Ga : S = 2 : 2.06 : 5.31 is very close to its stoichiometric value. The powder XRD results are shown in Fig. 2. The refined lattice parameters are $a = 3.718$ Å and $c = 15.242$ Å, close to previous parameters reported for polycrystal $Mn_2Ga_2S_5$.[34]

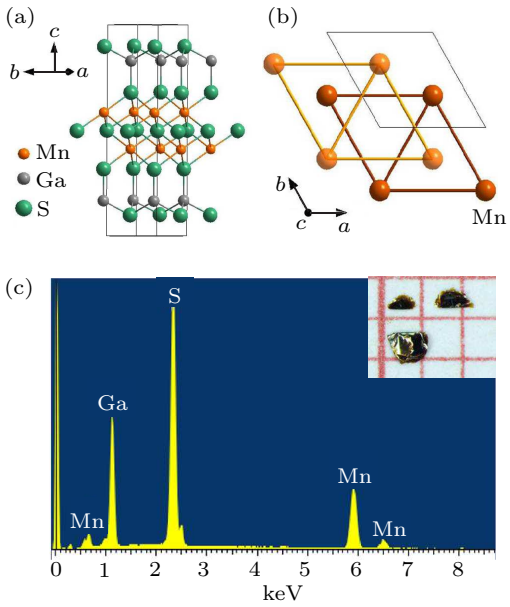


Fig. 1. (a) Crystal structure of $Mn_2Ga_2S_5$, showing a typical vdWs structure. Each unit cell contains double layers of Mn atoms. (b) Top view of the two sets of triangle Mn sublattice. Top set and bottom set are shown with different degrees of saturation. (c) EDX spectrum of $Mn_2Ga_2S_5$. The atomic ratio is determined to be 2 : 2 : 06 : 5 : 31, close to its stoichiometric value. Inset shows the optical image of several as-grown single crystals.

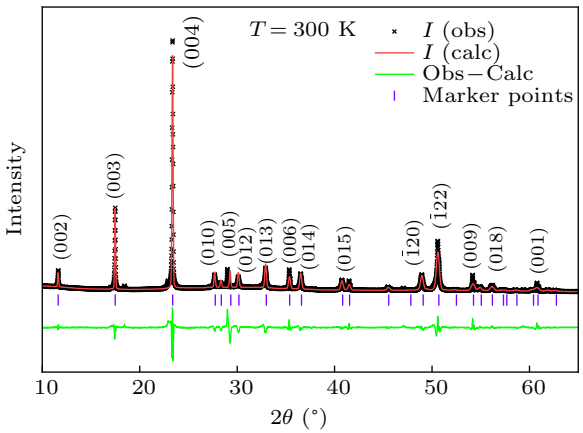


Fig. 2. Rietveld refinements of the powder XRD pattern for $Mn_2Ga_2S_5$ at 300 K.

We start by performing dc magnetization measurements on $Mn_2Ga_2S_5$. Figure 3(a) depicts the temperature-dependence of the magnetic susceptibility measured at applied magnetic fields of 500 Oe and 5000 Oe oriented perpendicular to the c axis with both zero-field-cooling (ZFC) and field-cooling (FC), respectively. Both FC and ZFC curves show highly coincident behavior above 12 K. At 500 Oe, the ZFC and FC curves bifurcate at $T_f = 12$ K for both in-plane and

out-of-plane (not shown here) directions, indicating a spin-freezing transition. Unlike $NiGa_2S_4$ or $FeGa_2S_4$,[24] this feature withstands relative strong magnetic fields. We find that the bifurcation at 5000 Oe shifts to 8.5 K with increasing fields, while the bending around 12 K can still be observed. In the high temperature region, the magnetic susceptibility decreases rapidly. As shown in Fig. 3(b), the inverse magnetic susceptibility $1/\chi$ is linear above 150 K, suggesting a Curie–Weiss paramagnetic state. There is a downward curving in the $1/\chi$ profile below 50 K, which is due to the formation of spin clusters.[35] By fitting the high temperature linear part of $1/\chi_{ab}$ to the Curie–Weiss law

$$\chi = \frac{C}{T-\theta_{\rm w}},$$

with C being the Curie constant and $\theta_{\rm w}$ the Curie–Weiss temperature, the effective moment is fitted as $\mu_{\rm eff} = 5.597\ \mu_{\rm B}/{\rm Mn}$, close to the expected value (5.92 $\mu_{\rm B}$) for high spin Mn^{2+} ions with $S = 5/2$. $\theta_{\rm w}$ is estimated to be as high as -260 K, leading to an empirical frustration index of $f = -\theta_{\rm w}/T_{\rm f} \approx 22$. The value is much larger than those in the homologous triangular spin-freezing systems $NiGa_2S_4$ and $FeGa_2S_4$ (around 10[24]), revealing that the sample is strongly frustrated.[36] The anisotropic ratio χ_{ab}/χ_c is closed to 1 for all temperatures, suggesting the overall interaction between Mn^{2+} is almost Heisenberg type.

Figures 3(c) and 3(d) show the field dependence of the magnetization at representative temperatures. The magnetization is not saturated at 7 T. When the magnetic field is along the c axis, we observe a small field hysteresis loop around ± 4 T which fades away above 5 K. The saturation magnetization for this low temperature ferromagnetic component is estimated to be around 0.025 $\mu_{\rm B}$/Mn, about 0.4% of the effective moment. An intuitive thinking is the inclusion of some magnetic impurity phase in the samples. However, possible impurity phases like $MnGa_2S_4$, MnS, MnS_2, Mn_2O_3, etc. all have $T_{\rm C}/T_{\rm N}$ well above 10 K,[37–40] whereas the hysteresis loops in our samples could only be observed below 5 K. We cannot rule out the possibility of an intrinsic, field induced weak ferromagnetism as competition between frustration and exchange interaction inside the vdWs bilayers may mimic some kind of canted antiferromagnetism.

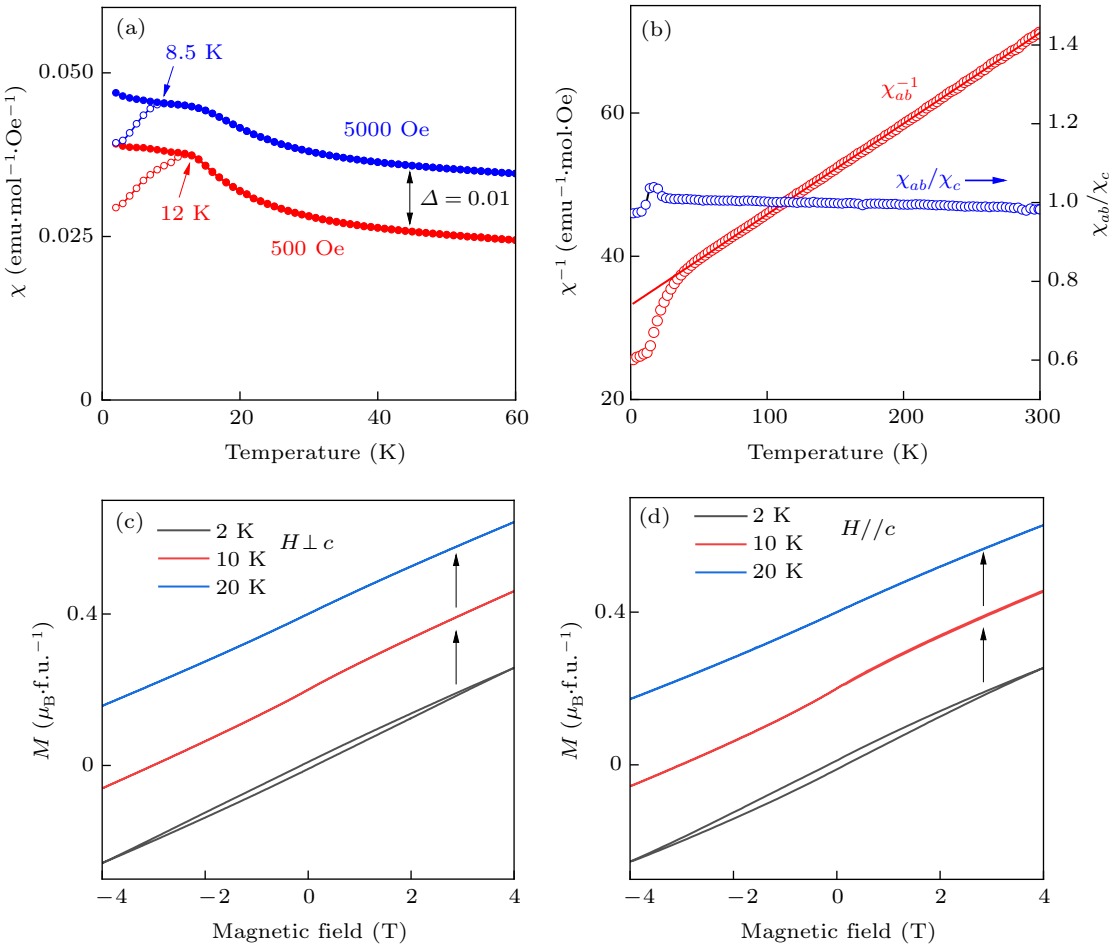


Fig. 3. (a) Temperature dependent magnetic susceptibility χ of $Mn_2Ga_2S_5$ with perpendicular ($H \perp c$) field configuration. The red and blue lines correspond to 500 Oe and 5000 Oe applied magnetic field, respectively. The field-cooling (solid circles) and zero-field-cooling (hollow circles) profiles bifurcate at low temperatures, typical of a spin freezing behavior. (b) The inverse magnetic susceptibility χ^{-1} (red line) and anisotropic ratio χ_{ab}/χ_c (blue line) obtained in the FC sequence at 500 Oe. (c) and (d) The field dependent magnetization curves with $H \parallel c$ and $H \perp c$ at representative temperatures. Curves are shifted vertically for clarity.

To shed light on the nature of magnetic ordering in the $Mn_2Ga_2S_5$, we also measure its specific heat in Fig. 4(a). The specific heat C_p shows neither a λ-like anomaly or any transition features around $T_f = 12$ K, which is consistent with features of spin glasses. The curves are also identical with different applied magnetic fields up to 14 T, meaning that the spin-disordered states are very insensitive to fields. As $Mn_2Ga_2S_5$ is a layered chalcogenide magnetic semiconductor/insulator, the electronic contribution to specific heat which arises from free charged carriers should be negligible. The specific heat of $Mn_2Ga_2S_5$ therefore consists of the lattice part C_{latt} and magnetic contribution C_{mag}, which is expressed by the following formula:[41,42]

$$C_p = C_{mag} + C_{latt},$$

where C_{mag} is the magnetic contribution to specific heat. For a rough estimation of the lattice contribution C_{latt}, the specific heat of the homologous nonmagnetic material $Zn_2In_2S_5$ is used as a reference.[24] The C_{latt} of $Mn_2Ga_2S_5$ is related to that of $Zn_2In_2S_5$ by a scale factor $\Theta_D(T) \propto M_0^{-1/2}V_0^{-1/3}$, where $\Theta_D(T)$, M_0 and V_0 are the Debye temperature, the molar mass and volume, respectively.[2] As shown in Fig. 4(b), C_{mag}/T of $Mn_2Ga_2S_5$ shows one broad peak at around 30 K, corresponding to the release of magnetic entropy above the spin-freezing transition. This is unlike the case of TM_2X_4 where Goldstone-type spin waves from 2D gapless linearly dispersive modes contribute another peak below T_f.[24,26,27] This substantial difference should arise from the complex exchange interaction host in the bilayered Mn lattice. Compared with the simple triangular T sublattice in TM_2X_4, $Mn_2Ga_2S_5$ possesses two extra interlayer coupling paths among Mn–S–Mn atoms: nearly rectangular paths between the nearest neighbor (NN) Mn sites and 180° paths connecting the second NN Mn sites. In this bilayer structure, these bonds happen to form four sublattices of a buckled honeycomb lattice.[24] According to the J_1–J_2 model on the honeycomb lattice,[43] the system exhibits Neel magnetic order at $J_2/J_1 \lesssim 0.2$ and collinear type at $J_2/J_1 \gtrsim 0.4$, while in the intermediate region a disordered ground state is expected. As no long-range order has been detected, the coupling in $Mn_2Ga_2S_5$ seems to be within this intermediate region.

In Fig. 4(b), we also observe a tiny peak around 5 K, which is also field independent up to 14 T. As we discuss above, this may be either from some impurity phase or from inherent weak ferromagnetism corresponding to the ferromagnetic-like component in M–H curves in Figs. 3(c) and 3(d), which deserves further studies in future.

We also estimate the magnetic entropy S_{mag} using the following thermodynamic relation:

$$S_{mag} = \int_0^T \frac{C_{mag}}{T}\,\mathrm{d}T.$$

As shown in Fig. 4(b), S_{mag} appears to be larger than the theoretical total entropy $R\ln(6)$ for $S = 5/2$ spin degree of freedom. This may be due to the involvement of orbital degree of freedom due to holes in the t_{2g} orbitals, similar to the case of $FeGa_2S_4$.[24]

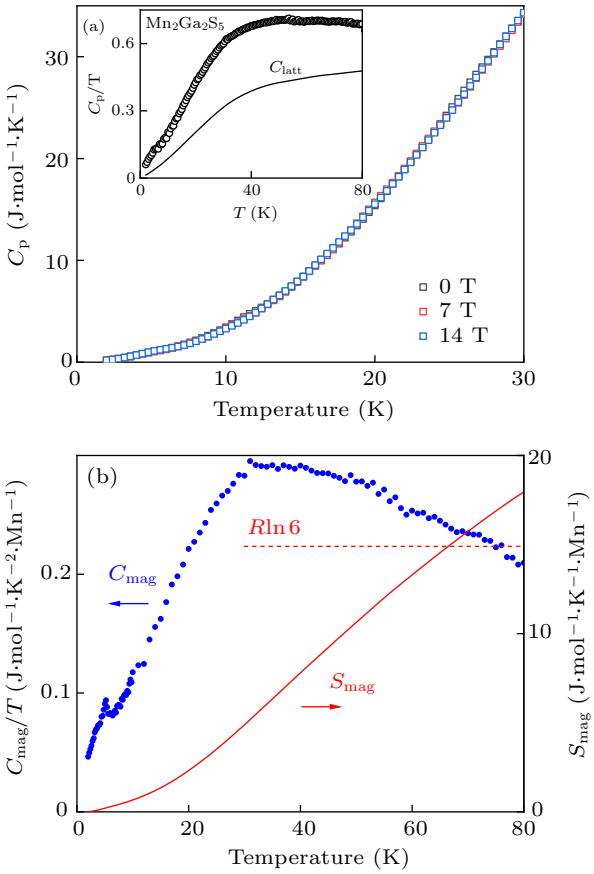


Fig. 4. (a) Specific heat C_p of $Mn_2Ga_2S_5$ at different magnetic fields up to 14 T. Inset: specific heat divided by temperature C_p/T at zero field and the lattice contribution C_{latt}/T estimated from the nonmagnetic homologous $Zn_2In_2S_5$.[24] (b) C_{mag}/T and the corresponding magnetic entropy S_{mag}.

Finally we discuss the ac magnetic susceptibility of $Mn_2Ga_2S_5$ at temperatures near the spin freezing temperature. Figure 5(a) shows the temperature dependent ac susceptibility from 13.7 Hz to 417 Hz, which is probed by a fixed ac magnetic field of 10 Oe. A peak reflecting the spin freezing temperature T_f is observed in the real part of the ac susceptibility, which shifts towards high temperatures with the enhanced ac frequency. In the empirical Vogel–Fulcher law,[44,45] T_f and the frequency f is related by

$$T_f = T_0 - \frac{E_a}{k_B}\frac{1}{\ln(\tau_0 f)},$$

where τ_0, E_a, and T_0 are the intrinsic relaxation time, the activation energy of the process, and the ideal glass temperature, respectively. As shown in Fig. 5(b), T_f is clearly linear with respect to $-1/\ln(\tau_0 f)$. The deduced $E_a/(k_B T_0) \sim 5$ is much larger than 1, confirming $Mn_2Ga_2S_5$ is unlike a canonical spin glass.[46] The shift of the peak temperature with respect

to frequency can also be described by the Mydosh parameter $(\Delta T_f)/(T_f \Delta \log \omega)$.[47] The obtained value for $Mn_2Ga_2S_5$ is 0.027 which is also larger than expected for a canonical spin glass (0.005 for CuMn and 0.0045 for AgMn).[44]

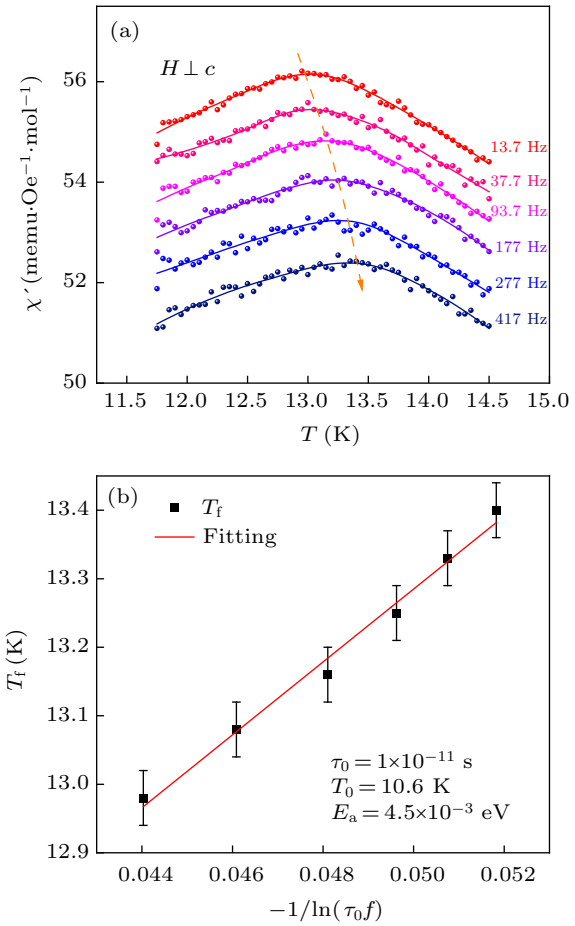


Fig. 5. (a) Temperature dependence of the real part of the ac magnetic susceptibility. The humps shift to higher temperatures with increasing frequencies. (b) Parametrization of the glassiness behavior in the fit to the Volger–Fulcher law. The relaxation time τ_0 is fixed to an empirical value of 1×10^{-11} s.[48]

4. Conclusion

We report the dc and ac magnetic susceptibility and specific heat measurements of the vdWs material $Mn_2Ga_2S_5$ featuring bilayered Mn triangular lattice. It is found that $Mn_2Ga_2S_5$ exhibits no long-range order down to 2 K. A spin freezing transition, which is observed as the bifurcation between field-cooling and zero-field-cooling dc magnetization and enhanced frequency dependence of ac magnetization, occurs at around 12 K, well below the Curie–Weiss temperature $\theta_w \sim -260$ K. This yields a frustration index of $f = -\theta_w/T_f \approx 22$, indicating the system is highly frustrated. The Mydosh parameter obtained from ac susceptibility measurements is also larger than what is expected for a canonical spin glass. The absence of a double-peak structure in magnetic specific heat compared with the TM_2S_4 compounds implies that the spin freezing behavior in $Mn_2Ga_2S_5$ is a result of the competition between exchange interactions and the bilayered 2D crystalline structure. The high magnetic interaction and strong frustration make $Mn_2Ga_2S_5$ a good candidate for studying the spin disorder state and the application of 2D layered magnetic material. Further neutron scattering measurement, nuclear magnetic resonance and muon spin resonance experiments can be useful to reveal detailed formation mechanism of the spin disorder state.

Acknowledgment

Project supported by the National Natural Science Foundation of China (Grant Nos. U1832214, 11774007, U2032213, and 12104461).

References

[1] Ramirez A 2001 *Handbook of Magnetic Materials* (Elsevier) Vol. 13 pp. 423–520
[2] Nakatsuji S, Nambu Y, Tonomura H, Sakai O, Jonas S, Broholm C, Tsunetsugu H, Qiu Y and Maeno Y 2005 *Science* **309** 1697
[3] Ye F, Ren Y, Huang Q, Fernandez-Baca J A, Dai P, Lynn J W and Kimura T 2006 *Phys. Rev. B* **73** 220404
[4] Kermarrec E, Marjerrison C A, Thompson C M, Maharaj D D, Levin K, Kroeker S, Granroth G E, Flacau R, Yamani Z, Greedan J E and Gaulin B D 2015 *Phys. Rev. B* **91** 075133
[5] Lotz B 2012 *Macromolecules* **45** 2175
[6] Canals B, Chioar I A, Nguyen V D, Hehn M, Lacour D, Montaigne F, Locatelli A, Mentes T O, Burgos B S and Rougemaille N 2016 *Nat. Commun.* **7** 11446
[7] Gardner J S, Gingras M J P and Greedan J E 2010 *Rev. Mod. Phys.* **82** 53
[8] Ramirez A P 1994 *Annu. Rev. Mater. Sci.* **24** 453
[9] Katsufuji T and Takagi H 2004 *Phys. Rev. B* **69** 064422
[10] Hagemann I S, Huang Q, Gao X P A, Ramirez A P and Cava R J 2001 *Phys. Rev. Lett.* **86** 894
[11] Wang R F, Nisoli C, Freitas R S, Li J, McConville W, Cooley B J, Lund M S, Samarth N, Leighton C, Crespi V H and Schiffer P 2006 *Nature* **439** 303
[12] Ramirez A P, Espinosa G P and Cooper A S 1992 *Phys. Rev. B* **45** 2505
[13] Wills A S, Harrison A, Ritter C and Smith R I 2000 *Phys. Rev. B* **61** 6156
[14] Petrenko O A, Ritter C, Yethiraj M and McK Paul D 1998 *Phys. Rev. Lett.* **80** 4570
[15] Gardner J S, Dunsiger S R, Gaulin B D, Gingras M J P, Greedan J E, Kiefl R F, Lumsden M D, MacFarlane W A, Raju N P, Sonier J E, Swainson I and Tun Z 1999 *Phys. Rev. Lett.* **82** 1012
[16] Ma Z, Ran K, Wang J, Bao S, Cai Z, Li S and Wen J 2018 *Chin. Phys. B* **27** 106101
[17] Wannier G H 1950 *Phys. Rev.* **79** 357
[18] Kurumaji T, Nakajima T, Hirschberger M, Kikkawa A, Yamasaki Y, Sagayama H, Nakao H, Taguchi Y, hisa Arima T and Tokura Y 2019 *Science* **365** 914
[19] Ye F, Fernandez-Baca J A, Fishman R S, Ren Y, Kang H J, Qiu Y and Kimura T 2007 *Phys. Rev. Lett.* **99** 157201
[20] Fritsch K, Ross K A, Granroth G E, Ehlers G, Noad H M L, Dabkowska H A and Gaulin B D 2017 *Phys. Rev. B* **96** 094414
[21] Dai J, Zhou P, Wang P S, Pang F, Munsie T J, Luke Graeme M, Zhang J S and Yu W Q 2015 *Chin. Phys. B* **24** 127508
[22] Nakatsuji S, Nambu Y, Onuma K, Jonas S, Broholm C and Maeno Y 2007 *J. Phys.-Condes. Matter* **19** 145232
[23] Takeya H, Ishida K, Kitagawa K, Ihara Y, Onuma K, Maeno Y, Nambu Y, Nakatsuji S, MacLaughlin D E, Koda A and Kadono R 2008 *Phys. Rev. B* **77** 054429
[24] Nakatsuji S, Tonomura H, Onuma K, Nambu Y, Sakai O, Maeno Y, Macaluso R T and Chan J Y 2007 *Phys. Rev. Lett.* **99** 157203
[25] Myoung B R, Lim J T and Kim C S 2017 *J. Magn. Magn. Mater.* **438** 121

[26] Dalmas de Réotier P, Yaouanc A, MacLaughlin D E, Zhao S, Higo T, Nakatsuji S, Nambu Y, Marin C, Lapertot G, Amato A and Baines C 2012 *Phys. Rev. B* **85** 140407

[27] Li K, Jin S, Guo J, Xu Y, Su Y, Feng E, Liu Y, Zhou S, Ying T, Li S, Wang Z, Chen G and Chen X 2019 *Phys. Rev. B* **99** 054421

[28] Smerald A, Ueda H T and Shannon N 2015 *Phys. Rev. B* **91** 174402

[29] Nambu Y and Nakatsuji S 2011 *J. Phys.-Condes. Matter* **23** 164202

[30] Tomita T, Nambu Y, Nakatsuji S, Koeda S, Hedo M and Uwatoko Y 2009 *J. Phys. Soc. Jpn.* **78** 094603

[31] Takubo K, Mizokawa T, Nambu Y and Nakatsuji S 2009 *Phys. Rev. B* **79** 134422

[32] Nakatsuji S, Nambu Y and Onoda S 2010 *J. Phys. Soc. Jpn.* **79** 011003

[33] Liao C, Jin Y, Zhang W, Zhu Z and Chen M 2020 *Chin. Phys. Lett.* **37** 107505

[34] Pardo M P, Fourcroy P H and Flahaut J 1975 *Mater. Res. Bull.* **10** 665

[35] Bao J K, Li L, Tang Z T, Liu Y, Li Y K, Bai H, Feng C M, Xu Z A and Cao G H 2015 *Phys. Rev. B* **91** 180404

[36] Ramirez A P 1994 *Annu. Rev. Mater. Sci.* **24** 453

[37] Lin M and Hacker H 1968 *Solid State Commun.* **6** 687

[38] Rimet R, Buder R, Schlenker C, Roques R and Zanchetta J 1981 *Solid State Commun.* **37** 693

[39] Heikens H, Wiegers G and van Bruggen C 1977 *Solid State Commun.* **24** 205

[40] Ahmad T, Ramanujachary K V, Lofland S E and Ganguli A K 2004 *J. Mater. Chem.* **14** 3406

[41] Bouvier M, Lethuillier P and Schmitt D 1991 *Phys. Rev. B* **43** 13137

[42] Gratz E, Loewenhaupt M, Divis M, Steiner W, Bauer E, Pillmayr N, Muller H, Nowotny H and Frick B 1991 *J. Phys.-Condes. Matter* **3** 9297

[43] Mezzacapo F and Boninsegni M 2012 *Phys. Rev. B* **85** 060402

[44] Mydosh J A 1993 *Spin Glasses: An Experimental Introduction* (CRC Press)

[45] Lubchenko V and Wolynes P G 2007 *Annu. Rev. Phys. Chem.* **58** 235

[46] Sahu B, Fobasso R D and Strydom A M 2022 *J. Magn. Magn. Mater.* **543** 168599

[47] Mydosh J A 1996 *J. Magn. Magn. Mater.* **157-158** 606

[48] Krizan J W and Cava R J 2014 *Phys. Rev. B* **89** 214401